Accepted Manuscript

Identification of novel PI3K inhibitors through a scaffold hopping strategy

Sonia Martínez González, Ana Isabel Hernández, Rosa María Álvarez, Antonio Rodríguez, Francisco Ramos-Lima, James R. Bischoff, María Isabel Albarrán, Antonio Cebriá, Elena Hernández-Encinas, Jennifer García-Arocha, David Cebrián, Carmen Blanco-Aparicio, Joaquín Pastor

PII: S0960-894X(17)30968-X
DOI: https://doi.org/10.1016/j.bmcl.2017.09.059
Reference: BMCL 25323

To appear in: *Bioorganic & Medicinal Chemistry Letters*

Received Date: 11 September 2017
Revised Date: 27 September 2017
Accepted Date: 28 September 2017

Please cite this article as: Martínez González, S., Hernández, A.I., Álvarez, R.M., Rodríguez, A., Ramos-Lima, F., Bischoff, J.R., Albarrán, M.I., Cebriá, A., Hernández-Encinas, E., García-Arocha, J., Cebrián, D., Blanco-Aparicio, C., Pastor, J., Identification of novel PI3K inhibitors through a scaffold hopping strategy, *Bioorganic & Medicinal Chemistry Letters* (2017), doi: https://doi.org/10.1016/j.bmcl.2017.09.059

Identification of novel PI3K inhibitors through a scaffold hopping strategy

Sonia Martínez González,[a] Ana Isabel Hernández,[a] Rosa María Álvarez,[a] Antonio Rodríguez,[a,Δ] Francisco Ramos-Lima,[a] James R. Bischoff,[a,§] María Isabel Albarrán,[a] Antonio Cebriá,[a] Elena Hernández-Encinas,[a] Jennifer García-Arocha,[a] David Cebrián,[a,¥] Carmen Blanco-Aparicio,[a] Joaquín Pastor[a*]

[a]Experimental Therapeutics Programme, Spanish National Cancer Research Centre (CNIO), C/Melchor Fernández Almagro 3, E-28029 Madrid, Spain
[*]Corresponding author: Tel.: +34 917328000; fax: +34 917328051. E-mail address: jpastor@cnio.es (J. Pastor).
[Δ]Present address: Centro de Investigacion Lilly S.A., Avda. de la Industria, 30, Alcobendas, E-28108, Madrid, Spain.
[§]Present address: Roche Innovation Center Basel, F. Hoffmann-La Roche Ltd, Grenzacherstrasse 124, 4070 Basel, Switzerland.
[¥]Present address: Pharmacology unit, Diseases of the developing world, GSK, C/ Severo Ochoa, 2, E-28760 Science to Business Technology Park, Spain.

Abstract: A scaffold hopping strategy, including intellectual property availability assessment, was successfully applied for the discovery of novel PI3K inhibitors. Compounds were designed based on the chemical structure of the lead compound ETP-46321, a potent PI3K inhibitor, previously reported by our group. The new generated compounds showed good *in vitro* potency and selectivity, proved to inhibit potently the phosphorylation of AKT^{Ser473} in cells and demonstrated to be orally bioavailable, thus becoming potential back-up candidates for ETP-46321.

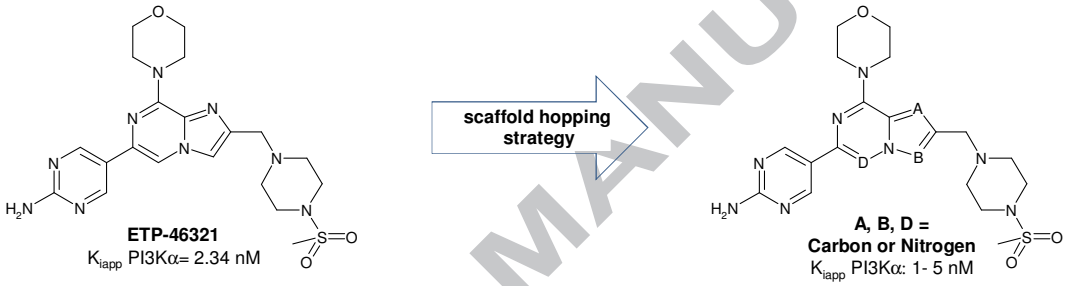

Keywords: Scaffold hopping, ETP-46321, PI3K inhibitors, back-up.

Scaffold hopping, a medicinal chemistry strategy based on the bioisosteric replacement of the core motif of a molecule, has become extensively applied in the drug discovery process in order to contribute to the development of novel chemical entities with high commercial value, if "intellectual property" aspects are included in the design. It has been widely used with the aim of improving potency, selectivity and/or ADMET properties of advanced compounds to generate potential "back-up" alternatives.[1] There are number of examples of successful drug discovery efforts employing this strategy. Among them, the discovery of Imigliptin, a novel selective DPP‑4 Inhibitor for the treatment of Type 2 Diabetes currently undergoing clinical trials which was identified via scaffold-hopping from Alogliptin, a marketed DPP-4 inhibitor.[2] More specifically, in the PI3K field, PQR309 (bimiralisib) initially inspired by ZSTK474 and structurally related with BKM120 (the pyrimidine central core of BKM120 was replaced by a triazine) was designed with the aim to avoid microtubule interaction of BKM120 and introduce moderate mTOR inhibition, among other factors. Bimiralisib is currently in phase II studies.[3]

Here, we present our successful application of this approach for the replacement of the imidazo[1,2-*a*] pyrazine core of ETP-46321 (Figure 1), a potent and orally bioavailable PI3K α, δ inhibitor identified in our group,[4] by other scaffolds in order to increase the structural diversity of our proprietary PI3K inhibitors while maintaining or improving its potency, selectivity and/or pharmacokinetic (PK) profile. The identification of the structurally diverse PI3K inhibitors presented herein has contributed to strengthening our competitive position by generating potential backup candidates of ETP-46321.

The development of inhibitors for the PI3K signaling pathway is an attractive area of research in oncology due to association of this pathway in several oncogenic malignancies.[5] Several drugs targeting PI3K, pan-PI3K and isoform-specific PI3K inhibitors, have been developed and are currently in clinical

trials in different phases of clinical development, alone or in combination with other agents, in both solid tumors and hematologic malignancies.[6] Additional studies for discovering novel structures of PI3K inhibitors with different isoform inhibition signatures are still needed to match the different molecular requirements of a number of tumor types in the context of personalized medicine treatments.

We based our design strategy assuming that the imidazo[1,2-*a*]pyrazine core of ETP-46321 plays mainly a scaffolding role to distribute important substituents for activity in the appropriate geometric configuration to reach the essential interactions with PI3K. We previously reported the proposed binding mode for ETP-46321 in PI3Kα,[7] based on the analysis of the structural information available for PI3K inhibitors bearing scaffolds with structural similarity and the high homology between PI3Kγ and PI3Kα.[8] Thus, the morpholinyl group establishes an H-bond with Val 851, while the 2-aminopyrimide moiety likely interacts with Asp 805 and probably with Lys 802 in PI3Kα. In this manner, the fragment methanesulfonyl-piperazine of ETP-46321 will be placed out toward the solvent accessible area. Based on this binding mode, we searched for alternative bicyclic scaffolds which allow a similar distribution of these key substituents in the ATP site of PI3K. Therefore, we decided to start exploring the potential of nitrogen movement from the N-1 position to N-3 resulting in pyrazolo[1,5-*a*]pyrazine derivative (**1**) and also the insertion of an additional nitrogen atom in the initial core leading to [1,2,4]triazolo[1,5-*a*]pyrazine (**2**) and imidazo[2,1-*f*][1,2,4]triazine (**3**) derivatives (Figure 1).

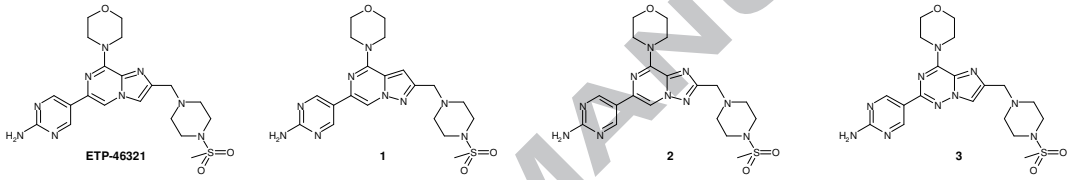

Figure 1. Scaffold-hopping drug design compounds.

The preparation of compounds **1-3** required the set up and optimization of three different synthetic routes.[9] The preparation of pyrazolo[1,5-*a*]pyrazine derivative **1** (Scheme 1) was carried out introducing the pyrazolo ring by N-alkylation reaction of commercial diethyl 3,5-pyrazoledicarboxylate with α-bromo ketone **9** in the presence of potassium carbonate as a base to give intermediate **10**. Intramolecular cyclization induced by reaction of **10** with ammonium acetate under microwave irradiation rendered pyrazolo[1,5-*a*]pyrazine bicycle **11** in 94% yield. A subsequent chlorination step with $POCl_3$ yielded the corresponding chlorinated pyrazolopyrazine intermediate which was treated with morpholine under nucleophilic aromatic substitution reaction conditions to give the expected compound **12** in good overall yield for both steps. The methanesulfonyl piperazine fragment was then introduced by a sequence of reactions over compound **12**: (i) reduction of the ester group with $LiAlH_4$ to produce the corresponding alcohol (ii) MnO_2 oxidation to obtain the aldehyde analogue and (iii) reductive amination of the aldehyde with 1-methanesulfonyl piperazine. Finally, the deprotection of the *p*-methoxybenzyl group of the 2-aminopyrimidine moiety in compound **13** was achieved using acidic conditions, thus leading to desired compound 5-[2-(4-Methanesulfonyl-piperazin-1-ylmethyl)-4-morpholin-4-yl-pyrazolo[1,5-*a*]pyrazin-6-yl]-pyrimidin-2-ylamine (**1**) (Scheme 1).

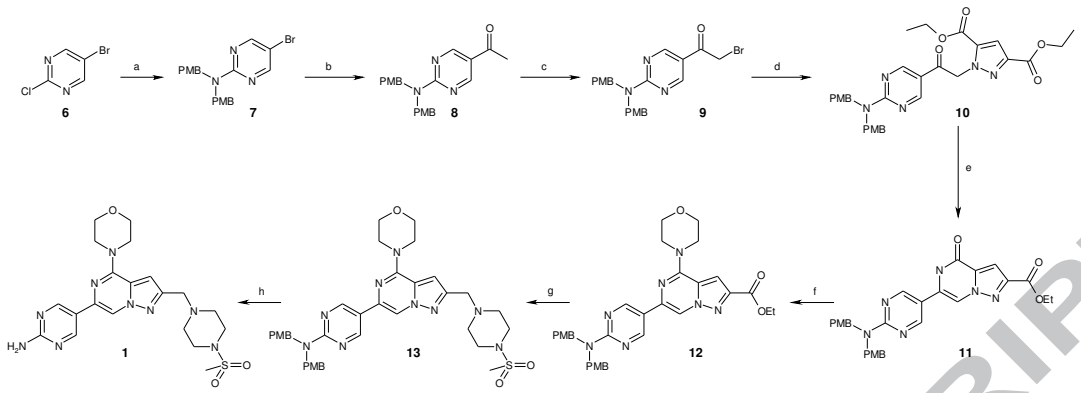

Scheme 1. Reagents and conditions: (a) Benzenemethanamine, 4-methoxy-*N*-[(4-methoxyphenyl)methyl]- hydrochloride, DIPEA, dioxane, 160 ºC, 1 h, 85%; (b) tributyl(1-ethoxyvinyl)tin (0.97 eq), $PdCl_2(Ph_3P)_2$ (0.05 eq), DMF, 100 ºC, 18 h, 66%; (c) i) trimethylsilyltrifluoromethane sulfonate, TEA, THF, 0 ºC, 2 h ii) NBS, 1 h, 0 ºC, quantitative (d) diethyl 3,5-pyrazoledicarboxylate, K_2CO_3 (1.2 eq), acetone, rt, 66%; (e) NH_4OAc (13 eq), EtOH, 150 ºC, 1 h, 94%; (f) i) $POCl_3$/*N*,*N*-dimethylaniline (12:1), 80 ºC, 16 h, ii) morpholine (20 eq), TEA (20 eq), dioxane, rt, 72 h, 61%; (g) i) $LiAlH_4$ 1M (2 eq), THF, 4 h, 0 ºC, 75%; ii) MnO_2 (15 eq), 1,2-DCE, rt, 5 h; iii) N-Ms-piperazine (2 eq), $NaBH(OAc)_3$ (1.5 eq), 1,2-DCE, AcOH (cat), 3 h, rt, 47%; (h) 1,2-DCE/TFA (2:1), H_2SO_4 (2 drops), rt, 12 h, 52%.

The preparation of the [1,2,4]triazolo[1,5-*a*]pyrazine derivative **2**, required the amination of the pyrazine ring as the key step for the introduction of the additional N atom. This amination step could be carried out directly by reaction of *o*-(mesitylsulfonyl)hydroxylamine (MSH) with morpholinyl derivate **15** to afford **17** in 87% yield. Alternatively, the reaction of precursor 3,5-dibromo-2-amine pyrazine (**14**) with MSH produced the aminated di-bromo derivative **16** (46% yield), which was further reacted with morpholine to reach the desired precursor **17**. Next, the base-catalyzed cyclization of **17** with 2-chloroacetaldehyde gave the corresponding 2-chloromethyl triazolopyrazine **18.** The N-alkylation with 1-methanesulfonyl piperazine in acetonitrile under reflux temperature afforded the expected 6-Bromo triazolopyrazine **19** in high yield. Finally, Palladium mediated Suzuki-Miyaura cross-coupling with 2-aminopyrimidine-5-boronic acid pinacol ester was carried out under microwave irradiation conditions to introduce the desired aminopyrimidine group at the 6-position of intermediate **19**, yielding the desired compound **2**, 5-[2-(4-Methanesulfonyl-piperazin-1-ylmethyl)-8-morpholin-4-yl-[1,2,4]triazolo[1,5-*a*]pyrazin-6-yl]-pyrimidin-2-ylamine, in an acceptable 21% yield (Scheme 2).

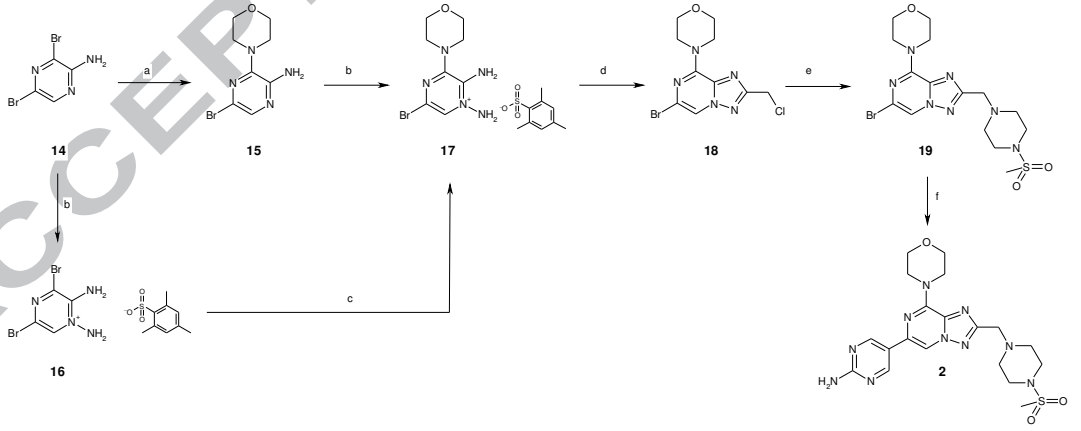

Scheme 2. Reagents and conditions: (a) morpholine, 120 ºC, 96%; (b) MSH, DCM, rt, 16 h, 46-87%; (c) morpholine (3 eq), DCM, rt, 1 h, quantitative; (d) 2-chloroacetaldehyde (10 eq), DCM, DBU (3 eq), rt, 18 h, 54%; (e) *N*-Ms-piperazine (1 eq), K_2CO_3 (1.5 eq), CH_3CN, 120 ºC, 16 h, 85%; (f) $PdCl_2(dppf)\cdot DCM$ (0.1 eq), aq. K_2CO_3, 2-aminopyrimidine-5-boronic acid pinacol ester (1.3 eq), DME, 130 ºC, 1 h, 21%.

The synthesis of imidazo[2,1-*f*][1,2,4]triazine **3** was initiated by the preparation of the key intermediate **21.** It was synthesized by acidic catalyzed condensation of ethyl bromopyruvate with 3,5-bis(methylthio)-

1,2,4-triazine-6-amine **20** followed by previously described nucleophilic aromatic substitution reaction with morpholine. The methanesulfonyl piperazine fragment was then introduced in the desired structure by reductive amination of the functionalized piperazine with aldehyde **22**, which was previously prepared by reduction of ester **21** with $LiAlH_4$ and subsequent oxidation of the intermediate alcohol with MnO_2. Finally, the Palladium mediated cross-coupling of the 6-methyl thioether **23** with 2-aminopyrimidine-5-boronic acid pinacol ester gave compound 5-[6-(4-Methanesulfonyl-piperazin-1-ylmethyl)-4-morpholin-4-yl-imidazo[2,1-*f*][1,2,4]triazin-2-yl]-pyrimidin-2-ylamine (**3**) with a very modest 7% yield (Scheme 3).

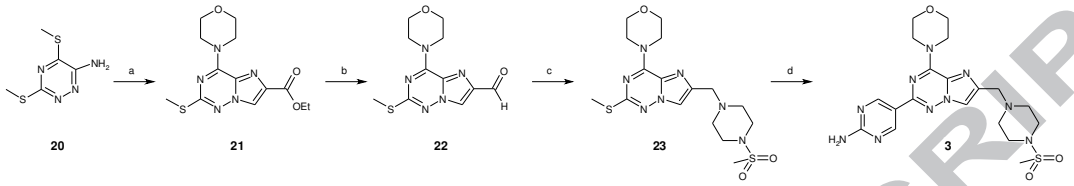

Scheme 3. Reagents and conditions: (a) (i) ethylbromopyruvate (5 eq), pTSOH (cat.), toluene, reflux, 18 h, (ii) morpholine (10 eq), AcCN, 85 ºC, 63%; (b) (i) $LiAlH_4$ 1M (2.5 eq), THF, 0 ºC, 1 h, 56%, (ii) MnO_2 (17 eq), $CHCl_3$, reflux, 2 h, 57%; (c) N-Ms-piperazine (2 eq), $NaBH(OAc)_3$ (1.3 eq), 1,2-DCE, trimethyl orthoformiate (10 eq), rt, 4 h, 99%; (d) $PdCl_2(dppf)$·DCM (0.1 eq), Cs_2CO_3 (2 eq), 2-aminopyrimidine-5-boronic acid pinacol ester (2 eq), DME, 130 ºC, 18 h, 7%.

Moreover, we decided to synthesize the chlorinated analogues of compounds **1** and **2** in order to block potential metabolic hot spots *in vivo* of their pyrazine rings, as we observed previously in compound **6** (compound **38** in reference 4a) where the 5-C chlorination of ETP-46321 improved the *in vivo* clearance from 0.56 to 0.39 L/h/Kg in compound **6**. As it can be deduced from their structure the free *para*-positions to the morpholine moiety (7-C in the pyrazolo[1,5-*a*]pyrazine and 5-C in the [1,2,4]triazolo[1,5-*a*]pyrazine) could be activated for potential oxidative metabolism by non microsomal enzymes. Furthermore, the introduction of a chlorine atom in these positions could increase the solubility of the resulting compounds due to the disruption of the planar conformation of the 2-aminopyrimidine moiety with respect to the central core. Thus, the Cl-derivatives **4** and **5** were prepared in moderate yields by taking advantage of the reactivity of the *p*-morpholinyl pyrazine moieties of compounds **1** and **2** in the presence of N-chlorosuccinimide (Scheme 4).

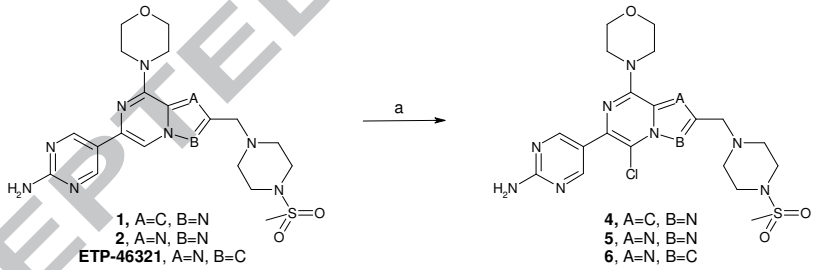

Scheme 4. Reagents and conditions: (a) NCS, DMF, rt, 16 h, 23-30%.

Once we had in hand the compounds **1-5** we proceeded to their evaluation as potential PI3K inhibitors. All of them demonstrated to be very potent PI3Kα inhibitors, in the same range than ETP-46321, showing single digit nanomolar values. Additionally, we determined their mTOR inhibition, PI3K isoforms profile and cellular activity based on the blockage of phosphorylation of AKT in U2OS cell line. The results were then compared to those of ETP-46321 (Table 1).

The five compounds (**1**-**5**) showed a good selectivity versus mTOR (IC_{50}> 1 μM), however, it is appreciated a slight impact of the scaffold replacement in their PI3K isoforms inhibition profiles. Thus, considering a given compound as selective when a selectivity ratio of 30-fold and higher is achieved (selectivity ratios for PI3K α are represented in Table 1 in brackets), compound **1** showed similar α,δ profile than ETP-46321 although its selectivity is not as pronounced, only 50 times selective versus β and γ, compared to the more than 70 fold selectivity obtained for ETP-46321. Interestingly, its chlorinated analogue, compound **4**, selective versus PI3K β, proved to be more active against the PI3K γ isoform. On

the other hand, the introduction of a Nitrogen atom more in the 5 or 6 membered ring of the central core (compounds **2** and **3**) decreased the activity of these analogues versus the β isoform (K_{iapp} = 155 and 388 nM respectively). A similar trend was also observed in the chlorinated compound **5** (PI3K β K_{iapp} = 285 nM). Overall, compounds **1**-**5** increased PI3Kγ activity compared to ETP-46321.

Finally, all of them showed similar or even better cellular activities than ETP-46321, AKT-P EC_{50} < 100 nM. Additionally, compounds **1**-**3** and **5** were tested in a representative 24 kinase panel showing a good selectivity profile, similar to ETP-46321, with values below 25% inhibition when tested at 1 μM.[14]

Table 1. Inhibition of PI3Kα, β, δ, γ, mTOR and cellular activity produced by compounds **1**-**5**.

Cpd	PI3Kα K_{iapp} nM[a]	PI3Kβ K_{iapp} nM[b]	PI3Kδ K_{iapp} nM[b]	PI3Kγ K_{iapp} nM[b]	mTOR IC_{50} nM[c]	AKT-P EC_{50} nM[d]
ETP-46321	2.34	170	14.2	179	4880	98[e]
		(x 72.6)	(x 6.1)	(x 76.5)	(x 2085)	
1	0.99	49.2	7.1	49.1	1700	30.5
		(x 49.7)	(x 7.2)	(x 49.6)	(x 1717)	
2	1.00	155	6.3	20.7	1260	87.2
		(x 155)	(x 6.3)	(x 20.7)	(x 1260)	
3	1.52	388	17.9	40.6	1840	52.8
		(x 255)	(x 11.8)	(x 26.7)	(x 1210)	
4	2.1	71.9	8.4	16.7	5410	34.5
		(x 33.4)	(x 3.9)	(x 7.8)	(x 2576)	
5	5.5	285	3.4	42.4	8170	68.6
		(x 51.8)	(x 0.6)	(x 7.7)	(x 1485)	

[a]The values reported are an average of two independent data points. Assay conditions described in reference 10 [b]The values are averages of two independent experiments performed in duplicate. Assay protocol reported in reference 11. In brackets are represented the selectivity fold versus alpha isoform. [C]The values reported are an average of two independent data points. Assay conditions described in reference 12. In brackets are represented the selectivity fold versus PI3K alpha [d]The values are averages of two independent experiments performed in duplicate with typical variation of less than ± 20%. Assay performed under C-Elisa format, conditions reported in reference 13. [e]When AKT phosphorylation inhibition was measured by Western blot analysis, AKT-P EC_{50}(ETP-46321) =8.3 nM (Reference 4) .

Next, the *in vitro* metabolic stability of our PI3K inhibitors was evaluated, after 30 minutes incubation with human and mouse liver microsomes. Compounds **1**-**5** exhibited good metabolic stability, higher than 95% of compound remained in all cases after incubation. These results were comparable to that obtained for ETP-46321 (Table 2). The inhibition of human CYP-P450 was also assessed and none of them, including ETP-46321, showed inhibition higher than 20% in any of the 5 CYPs isoforms profiled (CYP1A2, CYP2C9, CYP2C19, CYP2D6 and CYP3A4) suggesting low potential for CYP-inhibition dependent drug-drug interactions issues for them (Table 2). The *in vitro* solubility for these analogues was determined, resulting in lower solubility for compounds **1** and **3** in comparison with ETP-46321, whereas triazolopyrazines **2** and **5** seemed to be more soluble in the tested conditions. We also observed an improvement in the solubility of compound **4** when compared to **1,** confirming one of the potential benefits of chlorination cited before. Regarding their *in vitro* permeability, it was measured using a parallel artificial membrane assay (PAMPA). ETP-46321 and its analogues could be ranked as compounds with a medium passive permeability under these conditions, being the analogues somewhat better than ETP-46321, in particular the imidazotriazine **3**. Interestingly, none of the compounds showed significant blockade of the *h*ERG channel (IC_{50} > 30 μM) using a fluorescence polarization assay.[15]

Table 2. *In vitro* ADME parameters.

	ETP-46321	**Cpd 1**	**Cpd 2**	**Cpd 3**	**Cpd 4**	**Cpd 5**
	Imidazo-pyrazine	*Pyrazolo-pyrazine*	*Triazolo-pyrazine*	*Imidazo-triazine*	*7Cl-pyrazolopyrazine*	*5Cl-triazolopyrazine*
h, m LM[a]	100, 100	100, 100	97, 100	99, 100	97, 96	95, 100
CYPs[b]	<25	<25	<25	<25	<25	<25
Solubility[c]	50	10	100	10	100	100
PAMPA[d]	0.26	0.93	1.92	3.54	0.69	1.51

[a] Percent remaining after 30 min incubation. Assays performed in duplicates. Assay description in reference 16.
[b] Percent of CYPs inhibition at 10 µM test compound. Assays performed at Wuxi in duplicates (CYPs panel: 1A2, 2C9, 2C19, 2D6, 3A4).
[c] Solubility (µM). Assay description in reference 17.
[d] PAMPA Pe (10^{-6} cm/s). Assay description in reference 18.

Based on the general profile described above (Tables 1, 2), *in vivo* pharmacokinetic studies in BALB-C mice were performed with described PI3K inhibitors **1, 2, 4** and **5**. Compound **3** was not further characterized due to chemistry limitations for its scaling, which clearly might preclude its potential development.

The results of the PK studies after IV and PO administration of the different inhibitors are summarized in Table 3. The generated PK results for each compound contributed to build further their overall profiles to be used as criteria for the selection of these PI3K inhibitors as candidates for advanced *in vivo* studies and as potential back-up compounds of ETP-46321. Here, we need to note that the direct and exact comparison of the different PK parameters obtained for the compounds is not advisable. The compounds were tested at different doses in these studies and it is not possible to rule out the existence of dose-dependent effects which could affect results of total clearance, volume of distribution, half life and AUC.

Having this consideration into account, we can derive some conclusions from these studies. The total clearance after IV administration for compounds **1**, **4** and **5** is in the range of 0.65-0.75 L/h/Kg and close to the clearance observed for ETP-46321 (0.56 L/h/Kg) whereas the derivative **2** was profusely cleared from plasma (2.13 L/h/Kg). All the compounds displayed a clearance below the 50% of the hepatic blood flow for mice (5.5 L/h/Kg) therefore qualifying them as potential candidates for selection at this level.

Regarding the Vd (volume of distribution), their values represent (i) compounds with an even distribution profile between plasma and tissues, ETP-46321 and compound **1** with Vd: 0.8 and 0.6 L/Kg respectively, matching the total body water content of 0.6 L/Kg of the animals and (ii) compounds **2**, **4** and **5** with tendency to be distributed more preferentially outside the plasma compartment (Vd: 2.0, 1.24 and 1.61 L/Kg respectively). The AUC plasma levels for each compound reflect the effects of its clearance and distribution, thus compounds ETP-46321, **1**, **4** and **5** showed similar values when are taken proportionally to the IV dose employed for each compound, whereas triazolopyrazine **2** plasma levels are significantly lower. The described PI3K inhibitors demonstrated to be orally bioavailable as it can be observed by their %F values after PO administration (Table 3). Interestingly, all the compounds showed rapid absorption between 0.5-1.0 h (Tmax) and significant plasma levels (AUC) at the doses tested. Compounds **4** and **5** displayed higher plasma exposures when compared with their non-chlorinated analogues **1** and **2,** however only the 5-Cl triazolopyrazine **5** achieved comparable oral exposure to ETP-46321.

Table 3. Pharmacokinetic parameters[a]

	ETP-46321	Cpd 1	Cpd 2	Cpd 4	Cpd 5
IV					
dose IV (mg/Kg)	8	3	5	5	5
plasma $t_{1/2}$ (h)	1.36	0.51	0.26	0.61	1.81
Cl (L/h/Kg)	0.56	0.65	2.13	0.75	0.65
Vd (L/Kg)	0.8	0.6	2	1.24	1.61
AUCinf (ng.g/ml)	14185	5820	2658	8105	7733
PO					
dose (mg/Kg)	8	9	10	10	5
Tmax (h)	1	1	1	0.5	1
Cmax (ng/mL)	1132	938	674	1372	1051
AUCinf (ng.h/mL)	12573	5151	4691	6985	5651
plasma $t_{1/2}$ (h)	8.38	2.84	5.28	3.22	2.70
%F	88.6	29.5	88	43.1	73.1

[a] Pharmacokinetic parameters estimated by fitting the experimental data to a bicompartmental model using Winnonlin software. Plasma samples were obtained at 6/8 different times after IV/PO dosing and the concentration of compound in each sample was determined by LC/MS/MS. Each value represents the mean of 3 independent samples. Oral Formulation: 10% NMP/90% PEG300; IV Formulation: 10% NMP/50% PEG300/40% Saline Parameters: $t_{1/2}$ plasma half-life. Clearance (Cl). Volume of Distribution (Vd). AUC, area under curve. %F, oral bioavailability.

Nevertheless, it is important to highlight that the achieved oral plasma levels by all the compounds at the doses tested, which are far from the maximum tolerated ones (data not shown), clearly exceeded the concentration corresponding to their EC_{50} values for inhibition of AKT-P in cells (for more than 8 h for compound **1** where the PK was performed only up to 8 h and for more than 12 h for compounds **2**, **4** and **5** where PK was carried out up to 24 h) (Figure 2). Therefore, the described PI3K inhibitors qualify as candidates for further *in vivo* PK-PD and efficacy studies in mice.

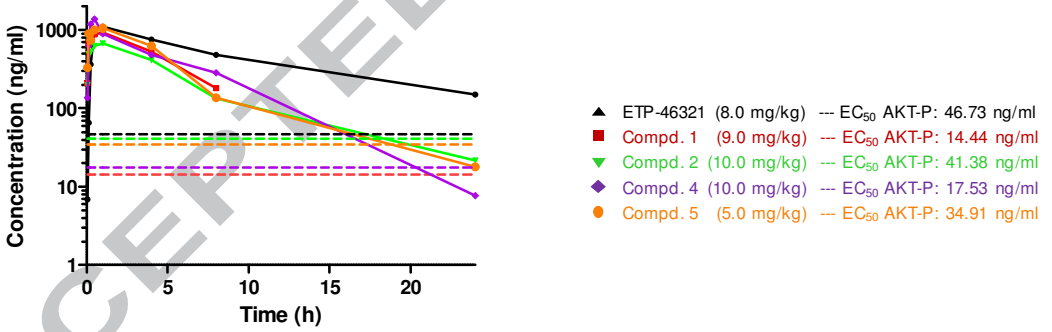

Figure 2. *In vivo* plasma concentration after oral administration of the compounds. In script lines are represented their EC_{50} values for inhibition of phosphorylation of AKT in U2OS cells.

In summary, utilizing a scaffold hopping approach to increase structural diversity, a series of different bicycles were identified. The pyrazolo[1,5-*a*]pyrazine, [1,2,4]triazolo[1,5-*a*]pyrazine and imidazo[2,1-*f*][1,2,4]triazine **1-5** derivatives were successfully synthesized and showed to be very potent PI3Kα inhibitors with diverse activity in the others PI3K isoforms. The compounds showed good selectivity versus mTOR and good modulation of AKT^{Ser473} phosphorylation in cells. Pharmacokinetic studies of compounds **1-2, 4-5** displayed favorable results to further characterize them in PK-PD and efficacy studies in different tumor mice models and to evaluate the potential of these products as back-up candidates of ETP-46321. The results of these studies will be reported in due course.

Acknowledgments

The Ministry of Science and Innovation (MICINN) of Spain supported this research through the project CIT-090100-2007-48. We thank Isabel Reymundo, Genoveva Mateos, María del Carmen Rodríguez de Miguel and Javier Klett for compound handling and sample preparation, and Manuel Urbano for data management.

[1] a) Brown, N; *Molecular Informatics* **2014**, *33* (6-7), 458-462. b) Sun, H.; Tawa, G.; Wallqvist, A. *Drug Discovery Today* **2012**, *17*, 310−324. c). Konkol, L. C.; Senter, T. J.; Lindsley, C. W. *Methods and Principles in Medicinal Chemistry* **2014**, *58*, (Scaffold Hopping in Medicinal Chemistry), 247-257. d) Schneider, G.; Schneider, P.; Renner, S. *QSAR Comb. Sci.* **2006**, *25*, 1162−1171. e) Southall, N. T.; Ajay. *J. Med. Chem*. **2006**, *49*, 2103−2109.

[2] Shu, C.; Ge, H.; Song, M.; Chen, J. H.; Zhou, H.; Qi, Q.; Wang, F.; Ma, X.; Yang, X.; Zhang, G.; Ding, Y.; Zhou, D.; Peng, P.; Shih, C. K.; Xu, J.; Wu, F. *ACS Med. Chem. Lett*. **2014**, *5*, 921−926.

[3] a) Beaufils, F.; Cmiljanovic, N.; Cmiljanovic, V.; Bohnacker, T.; Melone, A.; Marone, R.; Jackson, E.; Zhang, X.; Sele, A.; Borsari, C.; Mestan, J.; Hebeisen, P.; Hillmann, P.; Giese, B.; Zvelebil, M.; Fabbro, D.; Williams, R. L.; Rageot, D.; Wymann, M. P. *J. Med. Chem.* **2017**, *60*, 7524-7538. b) Bohnacker, T.; Prota, A. E.; Beaufils, F.; Burke, J. E.; Melone, A.; Inglis, A.J.; Rageot, D.; Sele, A. M.; Cmiljanovic, V.; Cmiljanovic, N.; Bargsten, K.; Aher, A.; Akhmanova, A.; Díaz, J.F.; Fabbro, D.; Zvelebil, M.; Williams, R. L.; Steinmetz, M. O.; Wymann, M. P. *Nature Comm.* **2017**, *8*, 1-17.

[4] a) Martínez González, S.; Hernández, A. I.; Varela, C.; Rodríguez-Arístegui, S.; Lorenzo, M.; Rodríguez, A.; Rivero, V.; Martín, J. I.; Saluste, C. G.; Ramos-Lima, F.; Cendón, E.; Cebrián, D.; Aguirre, E.; Gomez-Casero, E.; Albarrán, M.; Alfonso, P.; García-Serelde, B.; Oyarzabal, J.; Rabal, O.; Mulero, F.; Gonzalez-Granda, T.; Link, W.; Fominaya, J.; Barbacid, M.; Bischoff, J. R.; Pizcueta, P.; Pastor, J. *Bioorg. Med. Chem. Lett.* **2012**, *22* (10), 3460-3466. b) Granda, T.G.; Cebrián, D.; Martínez, S.; Villanueva Anguita, P.; Casas López, E.; Link, W.; Merino, T.; Pastor, J.; Serelde, B. G.; Peregrina, S.; Palacios, I.; Albarran, M. I.; Cebriá, A.; Lorenzo, M.; Alonso, P.; Fominaya, J.; Rodríguez López, A.; Bishoff, J. R. *Inv. New Drugs* **2013**, *31*(1), 66-76.

[5] a) Cantley, L. C. *Science* **2002**, *296*, 1655-1657. b) Engelman, J. A.; Luo, J.; Cantley, L. C. *Nat. Rev. Genet*. **2006**, *7*, 606–619. c) Engelman, J. A. *Nature Rev. Cancer* **2009**, *9*, 550-562. d) Ihle, N. T.; Powis, G. *Mol. Cancer Ther*. **2009**, *8*, 1-9. d) Fruman, D. A.; Rommel, C. *Nat. Rev. Drug Discov*. **2014**, *13*, 140-156.

[6] a) Ingrid A. Mayer, I. A.; Arteaga, C. L.; *Annu. Rev. Med*. **2016**, 67:11–28 b) Stark, A.-K.; Sriskantharajah, S.; Hessel, E. M.; Okkenhaug, K. *Curr. Opin. Pharmacol*. **2015**, *23*, 82-91 c) Yap, T. A.; Bjerke, L.; Clarke, P. A.; Workman, P. *Curr. Opin. Pharmacol.* **2015**, *23*, 98-107.

[7] Martínez González, S. ; Rodríguez-Arístegui, S.; Hernández, A.I.; Varela, C.; González Cantalapiedra, E.; Álvarez, R.M.; Rodríguez Hergueta, A.; Bischoff, J.R.; Albarrán, M.I.; Cebriá, A.; Cendón, E.; Cebrián, D.; Alfonso, P.; Pastor, J. *Bioorg. Med. Chem.* **2017**, *27* (11), 2536-2543.

[8] a) Huang, C. H. *Science* **2007**, *318*, 1744. b) Alaimo, P. J.; Knight, Z. A.; Shokat, K. M. *Bioorg. Med. Chem*. **2005**, *13*, (8), 2825.

[9] For detailed synthetic protocols: Pastor Fernández, J.; Martínez González, S.; Alvarez, Escobar, R.M.; Rodríguez, Hergueta, A.; Martín, Hernando, J.I.; Ramos, Lima, F.J. WO2011/089400 A1.

[10] The PI3Kα activity was measured by using the commercial ADP HunterTM Plus assay available from DiscoveRx, homogeneous assay to measure the accumulation of ADP, a universal product of kinase activity. The enzyme, PI3K (p110α/p85α) was purchased from Carna Biosciences and the assay was done following the manufacturer recommendation with slight modifications in the kinase buffer (50 mM HEPES,pH 7.5, 3 mM $MgCl_2$,100 mM NaCl, 1 mM EGTA, 0.04% CHAPS, 2 mM TCEP and 0.01 mg/ml BGG), and working at 10 nM PI3Kα (p110α/p85α) and at 50 μM of ATP concentration. Values were plotted against the inhibitor concentration and fitted to a sigmoid dose-response curve by using GraphPad Prism version 5.03 (GraphPad Software CA, USA). Values given are averages of two independent experiments performed in duplicate.

[11] The kinase activity of PI3K isoforms was measured by using the commercial PI3-kinase (h) HTRF™ assay available from Millipore, following the manufacturer recommendations. PI3Kα (p110α/p85α) and PI3Kδ (p110δ/p85α) were used at 100 pM; PI3Kβ (p110β/p85α) and PI3Kγ isoforms (p110γ) at 500 pM and 4 nM respectively. ATP concentration was 50 times K_MATP: 200 μM for PI3Kα and PI3Kδ, 250 μM for PI3Kβ and 100 μM for PI3Kγ. PIP2 was held at 10 μM. Values were normalized against the control activity included for each enzyme (i.e, 100% PI3K activity, without compound). These values were plotted against the inhibitor concentration and were fitted to a sigmoidal dose-response (variable slope) curve by using GraphPad Software. The obtained IC_{50} were converted to K_{iapp} according to Cheng-Prusoff equation for competitive inhibitors (Cheng, Y.; Prussoff, W.H. Biochem. Pharmacol. **1973**, *22*, 3099).

[12] mTOR (FRAP1), LanthaScreen™ Tb-anti-p4EBP1 (phosphor-threonine 46) and GFP-4E BP1 were purchased from Invitrogen. Reaction conditions used were those recommended by the manufacturer. Values given are averages of two independent experiments performed in duplicate.

[13] Cellular activity was measured as endogenous levels of phospho-Akt1 (Ser473) protein after serum stimulation in U2OS (osteosarcoma) cells growing in 0.1 % of FBS. Assay was run under C-Elisa format (Reagent: Supersignal Elisa Femto, purchased from Pierce). Values were plotted against the inhibitor concentration and fitted to a sigmoid dose-response curve using GraphPad Software.

[14] The values reported are an average of two independent data points for 24 kinases (AKT2, B_RAF^{V600E}, CHK1, CHK2, CK1α, CDK8, DYRK1A, EGFR, FAK, FGFR1, IGF1R, IKKβ, INSR, JAK2, KIT, MEK1, MET, PAK1, PDGFRα, PDK1, RPS6KA1, SGK1, SRC, VEGFR). Details of assay conditions can be found at www.proQinase.com.

[15] Predictor *h*ERG Assay test kits were obtained from Invitrogen (Carlsbad, CA). The binding assay was carried out

according to the kit instructions. Fluorescence polarization measurements were made using EnVision Microplate Reader from Perkin-Elmer Instruments. Polarization values were calculated automatically using Activity base Software. A description of the assay is published by Piper, D.R.; Duff, S.R.; Eliason, H.C.; Frazee, J.; Frey, E.A.; Fuerstenau-Sharp, Jachec, C.; Marks, B. D.; Pollok, B. A.; Shekhani, S.; Thompson, D.V.; Whitney, P.; Vogel, K.W.; Hess, S. D. *Assay & Drug Dev. Tech.* **2008**, *6*, 213.

[16] Human and mouse microsomal stability was determined using a single time point high throughput method. The final assay conditions were: 0.5 µM of the compounds, 0.5 mg/ml microsomal protein and NADPH-regenerating system incubated during 30 min at 37 ºC. Briefly, three separate 96-well plates containing the compounds, the microsomes and the NADPH regenerating enzymatic system (REG) were prepared. For the compound plate a solution of 50 µM of each compound in 25% DMSO in milliQ water was prepared. A second plate contained 0.5 mg/ml microsomes in 0.1 M potassium phosphate buffer pH 7.4 (BD Gentest) for each species (human, mouse, and rat). A third plate contained the REG was obtained by mixing solution A that contained 26 mM NADP+, 66 mM glucose-6-phosphate, and 66 mM $MgCl_2$ in H_2O and solution B consisted of 40 u/ml glucose-6-phosphate dehydrogenase in 5 mM sodium citrate. In the REG plate half of the plates contained the regenerating enzymatic system (positive wells) and half of the wells 0.1 M potassium phosphate buffer (negative wells). Parallel wells of each compound with the microsomes from all three species were prepared. The plates with the compounds, microsomes and REG were mixed. First, 139.5 µl of microsomes of each species were pipetted to a 96-well plate with Biomek FX automated liquid-handling instrument (Beckman Coulter). Next, 1.5 µl of compound solution were pipetted into the wells containing the microsomes. The plate with compounds and microsomes was mixed shortly. At last, 9 µl of enzyme solution or 0.1 M potassium phosphate buffer was pipetted into the 96-well plate. Once the enzyme was added 30 min incubation was started at 37 °C with 450 rpm shaking (Heidolph Inkubator 1000, Heidolph Titramax 1000). The reaction was stopped by adding 150 µl of acetonitrile containing 0.1% formic acid. The contents of the reaction plate wells were transferred to a NUNC deep 96-well plate containing 300 µl of acetonitrile with 0.1% formic acid. The plate was centrifuged for in 4 °C at 4000 rpm for 1 h with Eppendorf centrifuge 5810R. After incubation, 200 µl of supernatant was pipetted into two 96-well plates were analyzed with LC-MS/MS (an Agilent 1100 liquid chromatographer coupled to an API2000 (Applied Biosystems) triple quadrupole). The data was analyzed with Analyst 1.6.2 Software.

[17] The solubility of compounds was tested in phosphate buffered saline, pH 7.4. Compounds were inverted for 24 hours in test tubes containing 1–2 mg of compound with 1 mL of PBS. The samples were centrifuged and analyzed by HPLC (Agilent 1100 with diode-array detector). Peak area was compared to a standard of known concentration. In cases when the concentration was too low for UV analysis or when the compound did not possess a good chromophore, LC-MS/MS analysis was used.

[18] Parallel artificial membrane permeability assay (PAMPA) measures the capacity of molecule to cross an artificial plasma membrane. The assay was carried out in Corning Gentest Pre-Coated PAMPA Plate System (Corning). A system consisting of two plates, a 96-well receiver plate and a 96-well filter plate. The artificial plasma membrane of the filter plate consists of structured tri-layers of phospholipids. The compounds were dissolved in PBS. The concentration of compound in PBS was selected based on the kinetic solubility assay. The highest concentration soluble in PBS was used for PAMPA assay. First, 300 µl of each compound solution was pipetted into parallel wells of a 96-well receiver plate. Next, 200 µl of PBS was pipetted into the filter plate and the plate was placed on top of the receiver plate. The bottom plate with the compound acts as a donor and the top plate with the aqueous buffer as an acceptor. Propanolol (Sigma-Aldrich) 10 µM in PBS was used as a control with good permeability and Sorafenib (Sigma-Aldrich) 10µM in PBS as a control with poor permeability. The plates were incubated for 5 h at room temperature. After incubation 100 µl of sample was pipetted from each well of the receiver plate and filter plate to Waters 96-well. 300 µl of acetonitrile with 0.1% formic acid was added on the wells. Plate was mixed and further analyzed with LC-MS/MS. The data was acquired with Analyst 1.6.2 Software. Compound concentrations in donor plate and acceptor plate were obtained from the LC-MS/MS data analysis. Permeability was calculated using the equation $Pe= -Ln[1-C_A(t)/C_{equilibrium}]/A.(1/V_D+1/V_A).t$; where Pe is permeability (cm/s), $C_A(t)$ is a concentration of the compound in an acceptor well at time t (s), $C_D(t)$ is a concentration of the compound in a donor well at time t (s), A membrane area 0.3 cm^2, V_D is a donor well volume (0.3 ml), V_A is an acceptor well volume (0.2 ml), $C_{equilibrium}$ (t) is $[C_D(t).V_D+C_A(t).V_A]/(V_D+V_A)$. According to the manufacturer Corning Gentest™ the permeability of the compound is low if the permeability is lower than 15 nm/s and high if the permeability of the compound is greater than 15 nm/s.

Table 1. Inhibition of PI3Kα, β, δ, γ, mTOR and cellular activity produced by compounds **1**-**5**.

Cpd	PI3Kα K_{iapp} nM[a]	PI3Kβ K_{iapp} nM[b]	PI3Kδ K_{iapp} nM[b]	PI3Kγ K_{iapp} nM[b]	mTOR IC_{50} nM[c]	AKT-P EC_{50} nM[d]
ETP-46321	2.34	170	14.2	179	4880	98[e]
		(x 72.6)	(x 6.1)	(x 76.5)	(x 2085)	
1	0.99	49.2	7.1	49.1	1700	30.5
		(x 49.7)	(x 7.2)	(x 49.6)	(x 1717)	
2	1.00	155	6.3	20.7	1260	87.2
		(x 155)	(x 6.3)	(x 20.7)	(x 1260)	
3	1.52	388	17.9	40.6	1840	52.8
		(x 255)	(x 11.8)	(x 26.7)	(x 1210)	
4	2.1	71.9	8.4	16.7	5410	34.5
		(x 33.4)	(x 3.9)	(x 7.8)	(x 2576)	
5	5.5	285	3.4	42.4	8170	68.6
		(x 51.8)	(x 0.6)	(x 7.7)	(x 1485)	

[a]The values reported are an average of two independent data points. Assay conditions described in reference 10. [b]The values are averages of two independent experiments performed in duplicate. Assay protocol reported in reference 11. In brackets are represented the selectivity fold versus alpha isoform. [C]The values reported are an average of two independent data points. Assay conditions described in reference 12. In brackets are represented the selectivity fold versus PI3K alpha [d]The values are averages of two independent experiments performed in duplicate with typical variation of less than ± 20%. Assay performed under C-Elisa format, conditions reported in reference 13. [e]When AKT phosphorylation inhibition was measured by Western blot analysis, AKT-P EC_{50}(ETP-46321) =8.3 nM (Reference 4) .

Table 2. *In vitro* ADME parameters.

	ETP-46321	**Cpd 1**	**Cpd 2**	**Cpd 3**	**Cpd 4**	**Cpd 5**
	Imidazo-pyrazine	*Pyrazolo-pyrazine*	*Triazolo-pyrazine*	*Imidazo-triazine*	*7Cl-pyrazolopyrazine*	*5Cl-triazolopyrazine*
h, m LM[a]	100, 100	100, 100	97, 100	99, 100	97, 96	95, 100
CYPs[b]	<25	<25	<25	<25	<25	<25
Solubility[c]	50	10	100	10	100	100
PAMPA[d]	0.26	0.93	1.92	3.54	0.69	1.51

[a] Percent remaining after 30 min incubation. Assays performed in duplicates. Assay description in reference 16.

[b] Percent of CYPs inhibition at 10 µM test compound. Assays performed at Wuxi in duplicates (CYPs panel: 1A2, 2C9, 2C19, 2D6, 3A4).

[c] Solubility (µM). Assay description in reference 17.

[d] PAMPA Pe (10^{-6} cm/s). Assay description in reference 18.

Table 3. Pharmacokinetic parameters[a]

	ETP-46321	Cpd 1	Cpd 2	Cpd 4	Cpd 5
IV					
dose IV (mg/Kg)	8	3	5	5	5
plasma $t_{1/2}$ (h)	1.36	0.51	0.26	0.61	1.81
Cl (L/h/Kg)	0.56	0.65	2.13	0.75	0.65
Vd (L/Kg)	0.8	0.6	2	1.24	1.61
AUCinf (ng.g/ml)	14185	5820	2658	8105	7733
PO					
dose (mg/Kg)	8	9	10	10	5
Tmax (h)	1	1	1	0.5	1
Cmax (ng/mL)	1132	938	674	1372	1051
AUCinf (ng.h/mL)	12573	5151	4691	6985	5651
plasma $t_{1/2}$ (h)	8.38	2.84	5.28	3.22	2.70
%F	88.6	29.5	88	43.1	73.1

[a] Pharmacokinetic parameters estimated by fitting the experimental data to a bicompartmental model using Winnonlin software. Plasma samples were obtained at 6/8 different times after IV/PO dosing and the concentration of compound in each sample was determined by LC/MS/MS. Each value represents the mean of 3 independent samples. Oral Formulation: 10% NMP/90% PEG300; IV Formulation: 10% NMP/50% PEG300/40% Saline Parameters: $t_{1/2}$ plasma half-life. Clearance (Cl). Volume of Distribution (Vd). AUC, area under curve. %F, oral bioavailability.